JOURNAL OF MATERIALS SCIENCE 31 (1996) 2035–2042

Engineered flux pinning centres in Pb-doped high temperature superconducting "$Bi_2Sr_2CaCu_2O_8$" ceramics

P. MAJEWSKI, H.-L. SU, F. ALDINGER
Max-Planck-Institut für Metallforschung, Heisenbergstr. 5, 70569 Stuttgart, Germany

The Pb solubility of "$Bi_2Sr_2CaCu_2O_8$" is determined within the concentration range $Bi_{2.18-x}Pb_xSr_2CaCu_2O_{8+d}$ with $0 \leq x \leq 0.6$ and the temperature range from 800 to 900 °C. From a consideration of the Pb solubility in "$Bi_2Sr_2CaCu_2O_8$" a simple annealing procedure was developed to precipitate $(Pb, Bi)_4(Sr, Ca)_5CuO_{10+d}$ (451 phase) in high-temperature superconducting Pb-rich "$Bi_2Sr_2CaCu_2O_8$" ceramics. The precipitation results in a two-fold increase of the critical current density which is believed to express improved pinning properties of the superconducting ceramics. The microstructures of the samples with increased critical current density were studied with respect to the grain size and volume content of the 451 phase.

1. Introduction

"$Bi_2Sr_2CaCu_2O_8$" (2212 phase, T_c 94 K) exhibits weak internal pinning at temperatures above 30 K resulting in a decrease of the critical current density of more than two orders of magnitude in an applied magnetic field of about 1 T [1–3]. This behaviour hinders the application of the 2212 phase material in devices under magnetic fields. In different low and high temperature superconducting materials it has been shown that the pinning force can be increased, e.g. by introduction of secondary phases (e.g. Ta in Nb_3Sn, [4, 5]), by increasing the dislocation density [6, 7], by increasing the defect density by ion radiation [8–10] and by an optimization of the design of superconducting wires, e.g. NbTi multifilament wires [11]. Based on the observation of Murakami *et al.* [12, 13] who increased the pinning of Y–Ba–Cu–O ceramics by the introduction of inclusions of the secondary phase Y_2BaCuO_5, several investigations [14, 15] have claimed that secondary phases, e.g. Ca_2CuO_3, increase the pinning of 2212 and 2223 phase ("$Bi_2Sr_2Ca_2Cu_3O_{10}$") ceramics. However, the grains of ceramics prepared by powder technology are much too large (1–100 μm) to act as effective pinning centres which, in order to be most effective, should not exceed 10 nm due to the very small coherence length of the high-temperature superconducting phases [16–22]. In previous studies it has been demonstrated that precipitation of secondary phases in "$Bi_2Sr_2CaCu_2O_8$" originating from the temperature dependent Sr and Ca solubility results in an increase of the pinning properties [23–26]. In this work a processing route is presented to create enhanced pinning properties by precipitation of secondary phases using the temperature dependent Pb solubility of the 2212 phase. For this processing the phase relations of the Pb-doped 2212 phase were determined within the temperature range of 750 to 900 °C and the concentration range $Bi_{2.18-x}Pb_xSr_2CaCu_2O_{8+d}$ with $0 \leq x \leq 0.6$.

2. Experimental details

Samples have been prepared with the composition $Bi_{2.18-x}Pb_xSr_2CaCu_2O_{8+d}$ using Bi_2O_3, PbO, $SrCO_3$, $CaCO_3$ and CuO as starting materials (purity 99%). The mixed and ground powders were calcined at 750, 800 and 820 °C each for 24 h and pressed into cylindrical pellets. For the determination of the Pb solubility of the 2212 phase the pellets were sintered at 800 to 900 °C in air for 120 h with intermediate grinding and pressing and furnace cooled to room temperature with a cooling rate of about 10 K min^{-1}. For the precipitation of secondary phases, samples with the composition $Bi_{1.98}Pb_{0.2}Sr_2CaCu_2O_{8+d}$ were sintered at 850 °C for 120 h with intermediate grinding and pressing and furnace cooled to room temperature (10 K min^{-1}). Subsequently, the samples were annealed at 800 °C in air for 12 to 216 h and finally furnace cooled to room temperature (10 K min^{-1}).

The critical current densities of the pellets have been obtained by measuring the magnetic susceptibility at 30 K up to 1 T and calculating J_c from these data using Bean's model [27] and considering the volume of the samples. The magnetic susceptibility has been measured at 30 K, as at this temperature an increase of the pinning properties is expected to become most pronounced, because the transformation of the three-dimensional flux line lattice into a quasi two-dimensional pancake vortex has not occurred at that temperature and the pinning force of point defects, e.g. vacancies, is believed to be less effective at that temperature [16–22]. The accuracy of these

0022–2461

measurements is about ± 1–2%. The critical temperatures (onset) of the pellets have been determined by a.c. susceptibility measurements (accuracy: ± 1 K). Phase identification has been performed using electron microscopy with energy dispersive X-ray analysis (EDX) and X-ray diffraction (XRD) measurements. The Pb solubility has been determined by EDX (20 kV, using the Bi*L* and Pb*L* lines). The use of the Bi*M* and Pb*M* lines resulted in an overestimation of the Pb content at high Bi contents due to the overlapping of the *M*-lines in the EDX spectrum. The volume contents of the 4 5 1 phases were determined by point counting using SEM/BSE images where the white 4 5 1 grains easily can be distinguished from the grey 2 2 1 2 matrix. The accuracy is about ± 2 vol %. However, due to the limited resolution of the scanning electron microscope, grains with a size below 300 nm cannot be identified. Therefore, a systematical error for this method has to be taken into account. Nevertheless, the estimations of the volume content of the 4 5 1 phase from XRD pattern almost fit with the data given by point counting. The grain size of the 4 5 1 phase were measured using SEM/BSE images. About 250 grains of each sample were measured.

3. Results

The 2 2 1 2 phase exhibits a temperature dependent Pb solubility which is maximum at about 850 °C in air and decreases with increasing, as well as, decreasing temperatures (Fig. 1). With increasing temperatures the 2 2 1 2 phase decomposes forming a Pb-rich liquid with the approximate composition $Bi_{1.3}Pb_{1.3}Sr_1Ca_1Cu_1O_x$ and (Sr, Ca)CuO_2 with Sr:Ca ≈ 1:1 as determined from EDX analysis (Fig. 2). With increasing Pb content the formation of $(Sr, Ca)_{14}Cu_{24}O_{41-x}$ (Sr:Ca ≈ 1:1) besides (Sr, Ca)CuO_2 and a liquid was observed.

At lower temperatures, the 2 2 1 2 phase decomposes forming $(Pb, Bi)_4(Sr, Ca)_5CuO_{10+x}$ (4 5 1 phase). The crystal structure of this phase was determined to be hexagonal (Fig. 3 and Table I) with $a = b = 997$ pm and $c = 349.2$ pm which confirms the results of [28, 29]. Ca_2PbO_3 has not been observed within the range of concentration and temperature. However, it is believed that Ca_2PbO_3 is stable at lower temperature, because it is observed after calcining of the powders. During sintering the phase disappears due to the formation of the 2 2 1 2 and 4 5 1 phases. Therefore, the existence of Ca_2PbO_3 in the prepared sample indicates that the sample is still not in a thermodynamic equilibrium. The Sr to Ca ratio of the 2 2 1 2 phase of all samples is about 2:1 as determined from EDX analysis. The Pb to Bi and the Sr to Ca ratio of the 4 5 1 phase is about 4:1 and 1:1, respectively.

The annealing at 800 °C of the samples with the composition $Bi_{1.98}Pb_{0.2}Sr_2CaCu_2O_{8+d}$ sintered at 850 °C results in the formation of 4 5 1 phase (Figs 4–7). The precipitation of the 4 5 1 phase appears to be completed after about 50 h of post annealing as indicated in Fig. 8. At this time the 4 5 1 phase is fully precipitated and its volume content is defined by the

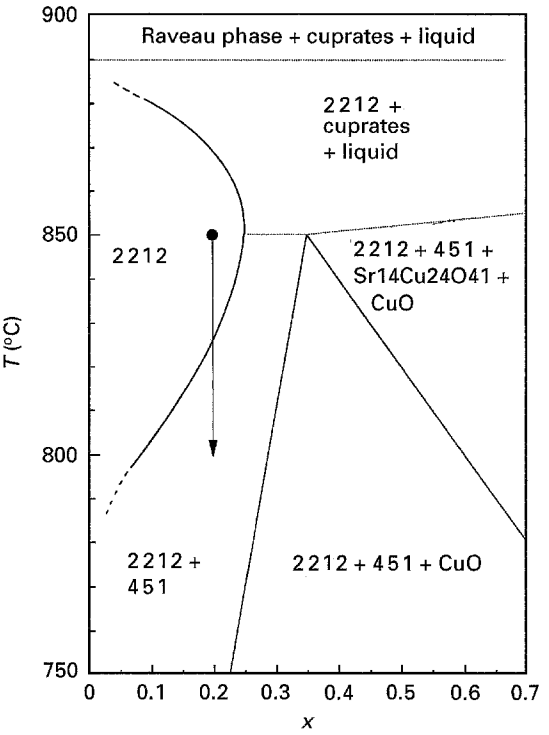

Figure 1 Section through the quasiquinary system Bi_2O_3–PbO–SrO–CaO–CuO within the concentration range $Bi_{2.18-x}Pb_xSr_2CaCu_2O_{8+d}$ with $0 \leq x \leq 0.6$ including the performed annealing step (arrow) to precipitate 4 5 1 phase.

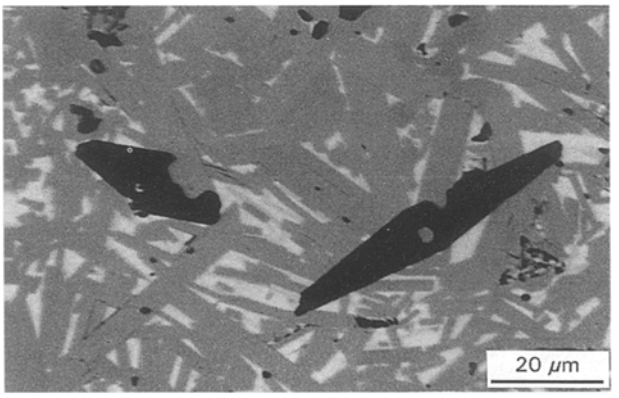

Figure 2 SEM/BSE image of a sample with the composition $Bi_{1.8}Pb_{0.38}Sr_2CaCu_2O_{8+d}$ annealed at 886 °C. White: liquid; grey: 2 2 1 2 phase; black: (Sr, Ca)CuO_2.

phase relations within the system Bi_2O_3–PbO–SrO–CaO–CuO at this temperature and at this cation concentration. With further annealing only grain coarsening of the 4 5 1 crystals occurs.

The T_c of the samples (82 K) and the trend of the susceptibility lines have not been changed significantly by the post annealing (Fig. 9). Therefore, the increased pinning cannot be caused by an increased critical temperature of the 2 2 1 2 phase or an increased superconducting volume fraction at 30 K.

In Fig. 10 J_c at different applied magnetic fields is plotted versus the annealing time at 30 K. The diagram shows a pronounced maximum for J_c at about 24 h of post annealing which indicates improved pinning properties.

The J_c versus B plot of the as-sintered and the 24 h post-annealed sample clearly shows that the J_c values

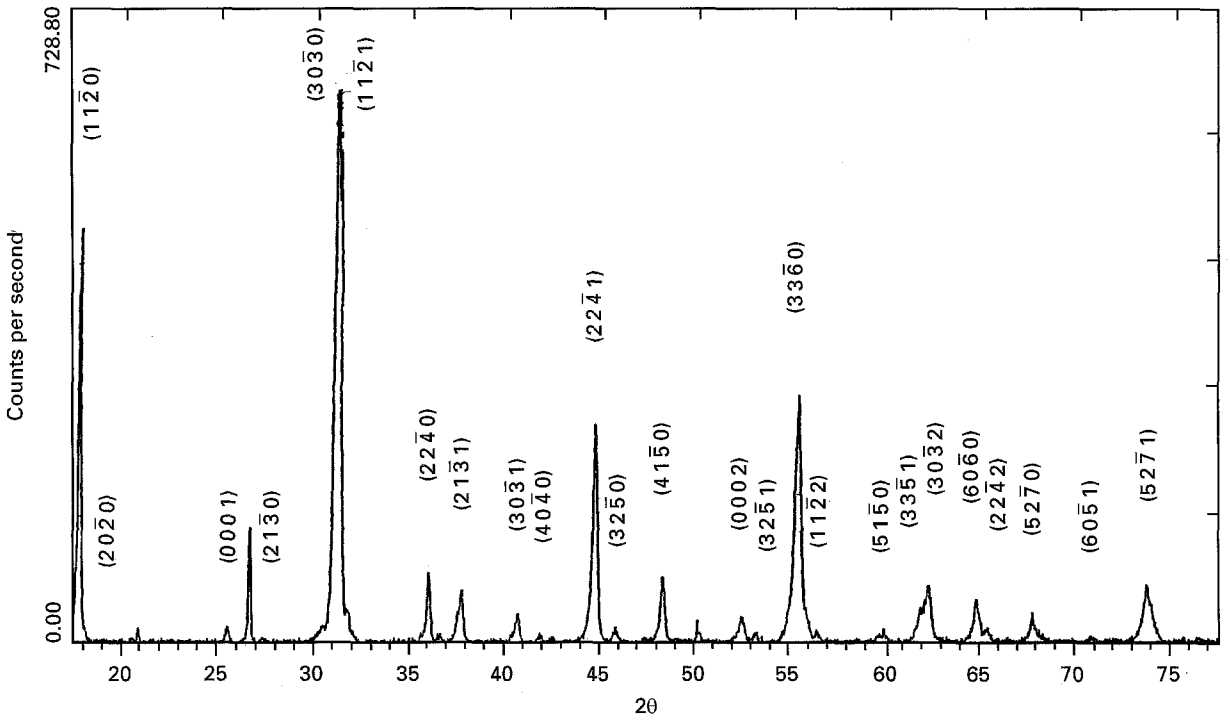

Figure 3 X-ray diffraction pattern of the 4 5 1 phase. Calculated and observed data are given in Table I.

TABLE I Crystallographic data (see Fig. 3)

2θ (°) observed	*d* (nm) observed	2θ (°) calculated	*d* (nm) calculated	(*hkl*)	(*hkil*)
17.825	0.4972	17.777	0.4985	(1 1 0)	(1 1 $\bar{2}$ 0)
20.605	0.4307	20.555	0.4317	(2 0 0)	(2 0 $\bar{2}$ 0)
25.577	0.3480	25.482	0.3492	(0 0 1)	(0 0 0 1)
27.395	0.3253	27.304	0.3263	(2 1 0)	(2 1 $\bar{3}$ 0)
31.138	0.2870	31.046	0.2878	(3 0 0)	(3 0 $\bar{3}$ 0)
31.317	0.2854	31.244	0.2860	(1 1 1)	(1 1 $\bar{2}$ 1)
36.071	0.2488	36.002	0.2492	(2 2 0)	(2 2 $\bar{4}$ 0)
37.785	0.2379	37.693	0.2384	(2 1 1)	(2 1 $\bar{3}$ 1)
40.701	0.2215	40.583	0.2221	(3 0 1)	(3 0 $\bar{3}$ 1)
41.867	0.2156	41.812	0.2159	(4 0 0)	(4 0 $\bar{4}$ 0)
44.740	0.2024	44.625	0.2029	(2 2 1)	(2 2 $\bar{4}$ 1)
45.839	0.1978	45.767	0.1981	(3 2 0)	(3 2 $\bar{5}$ 0)
48.349	0.1881	48.260	0.1884	(4 1 0)	(4 1 $\bar{5}$ 0)
52.520	0.1741	52.347	0.1746	(0 0 2)	(0 0 0 2)
53.245	0.1719	53.109	0.1723	(3 2 1)	(3 2 $\bar{5}$ 1)
55.441	0.1656	55.232	0.1662	(3 3 0)	(3 3 $\bar{6}$ 0)
56.441	0.1629	55.728	0.1648	(1 1 2)	(1 1 $\bar{2}$ 2)
59.983	0.1541	59.564	0.1551	(5 1 0)	(5 1 $\bar{6}$ 0)
61.936	0.1497	61.773	0.1501	(3 3 1)	(3 3 $\bar{6}$ 1)
62.31	0.1489	62.120	0.1493	(3 0 2)	(3 0 $\bar{3}$ 2)
64.830	0.1437	64.723	0.1439	(6 0 0)	(6 0 $\bar{6}$ 0)
65.444	0.1425	65.173	0.1430	(2 2 2)	(2 2 $\bar{4}$ 2)
67.805	0.1381	67.713	0.1383	(5 2 0)	(5 2 $\bar{7}$ 0)
70.846	0.1329	70.748	0.1331	(6 0 1)	(6 0 $\bar{6}$ 1)
73.796	0.1283	73.628	0.1285	(5 2 1)	(5 2 $\bar{7}$ 1)

of the 24 h annealed sample are significantly higher compared to those of the as-sintered sample (Fig. 11).

Fig. 12 shows the grain size distribution curves of the 4 5 1 phase precipitates of different samples. It is clearly seen that the grain size of the precipitates increases with increasing annealing time. Precipitates smaller than about 300 nm have not been determined due to the limited resolution of the scanning electron microscope. To overcome this drawback TEM studies of a 48 h annealed sample were performed revealing the existence of 4 5 1 precipitates with a grain size below 300 nm (Fig. 13).

Fig. 14 shows that the relation of the mean grain size of the samples and the square root of the annealing time exhibits a linear dependence, which suggests a diffusion controlled growth of the precipitates. Considering this diagram, it follows that a mean grain size of the precipitates of about 10 nm can be maintained at annealing times of less than 10 min. However,

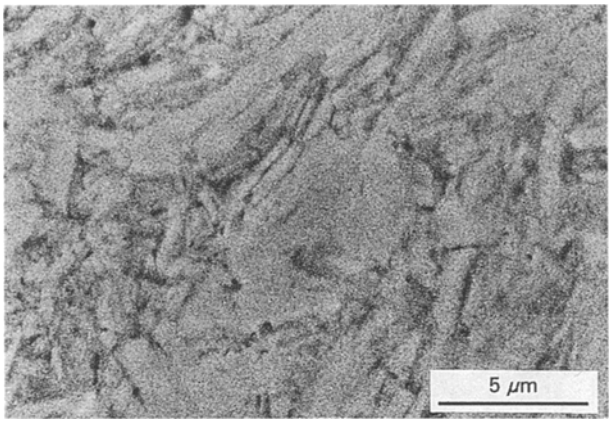

Figure 4 SEM/BSE image of the single phase as-sintered sample. Black dots: pores

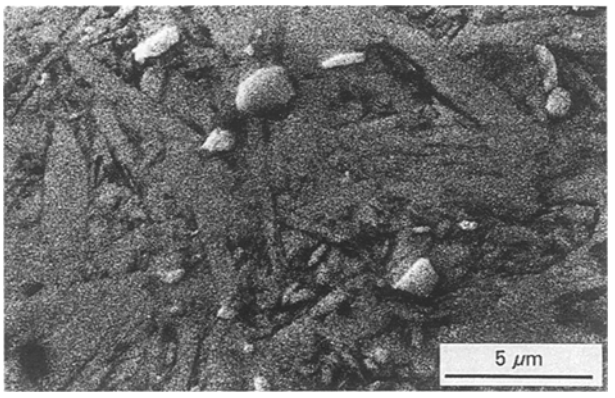

Figure 5 SEM/BSE image of the 216 h annealed sample. White: 4 5 1 phase; grey (matrix): 2 2 1 2 phase; black dots: pores.

considering Fig. 10 a significant shift of the pinning properties cannot be expected for an annealing time of only 10 min.

The grain size of the 2 2 1 2 phase appears to be unaffected by the annealing as observed by electron microscopy (Figs 4 and 5).

4. Discussion

The Pb solubility of the 2 2 1 2 phase was found to be slightly lower compared to previous studies [30]. This is possibly due to the fact that the Pb solubility of the phase is a function of the Bi content of the phase which would agree with the observed relation between the Bi content and the Pb solubility of the 2 2 2 3 phase ($[Bi, Pb]_{2+x}Sr_2Ca_2Cu_3O_{10+d}$) [31].

The XRD pattern of the 4 5 1 phase is very similar to that of Ca_2PbO_3. Therefore, using the XRD pattern for the determination of the phase content, Ca_2PbO_3 and the 4 5 1 phase can easily be confused. However, the results do not provide evidence that Ca_2PbO_3 does not exist within the system at temperatures above 800 °C in air. As the 4 5 1 phase basically is a Pb–Sr–Cu–O compound the existence region for Ca_2PbO_3 under such conditions can be expected at Ca-rich concentrations.

The observed increase of J_c during precipitation of the 4 5 1 phase agrees with the observed increase of J_c during precipitation of secondary phases in Ca- and Sr-rich 2 2 1 2 phase ceramics reported in [23–26]. The fact that the chemical composition of the 2 2 1 2 phase of the different experiments and the applied annealing procedures are different indicates that a uniform effect increases the J_c of these ceramics.

As the J_c of the samples is calculated from magnetization measurements, it has to be taken into account that the intergrain currents, as well as the intragrain currents within isolated superconducting regions, e.g. grains or cluster of grains, contribute to the overall magnetization of the samples. An increase of the intergrain current can be provided by an increase of

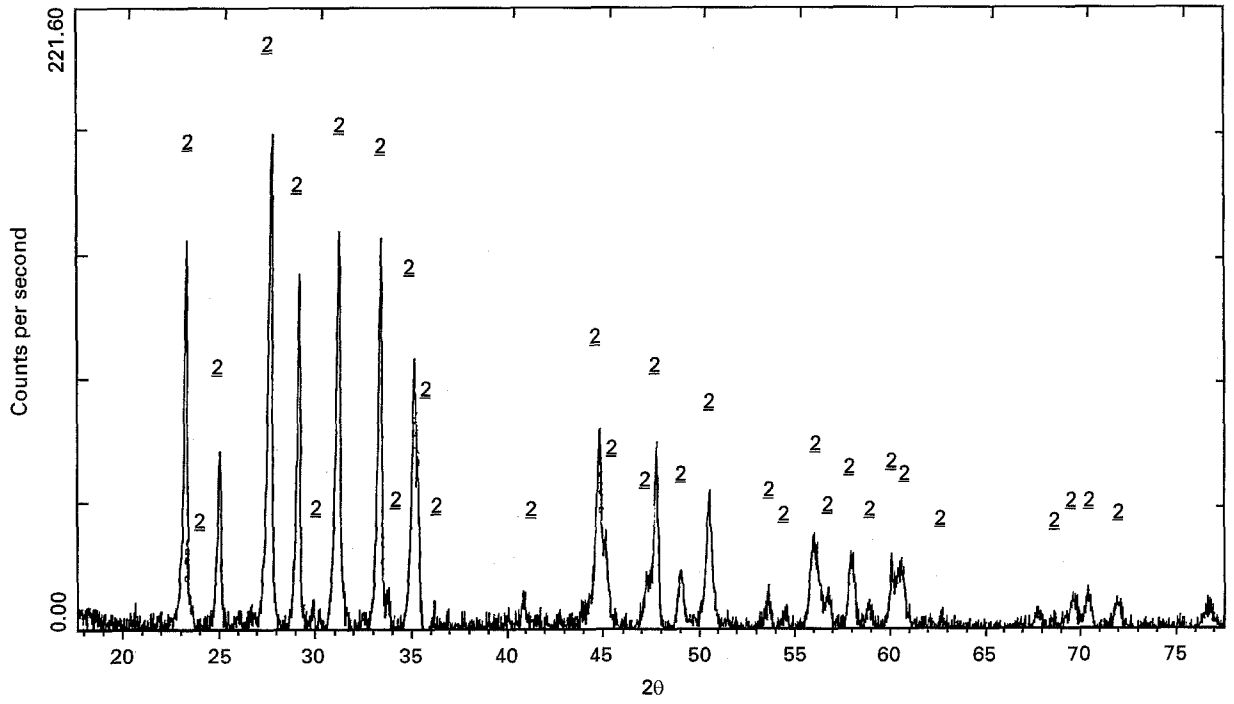

Figure 6 XRD-pattern of the as-sintered sample. 2: 2 2 1 2 phase.

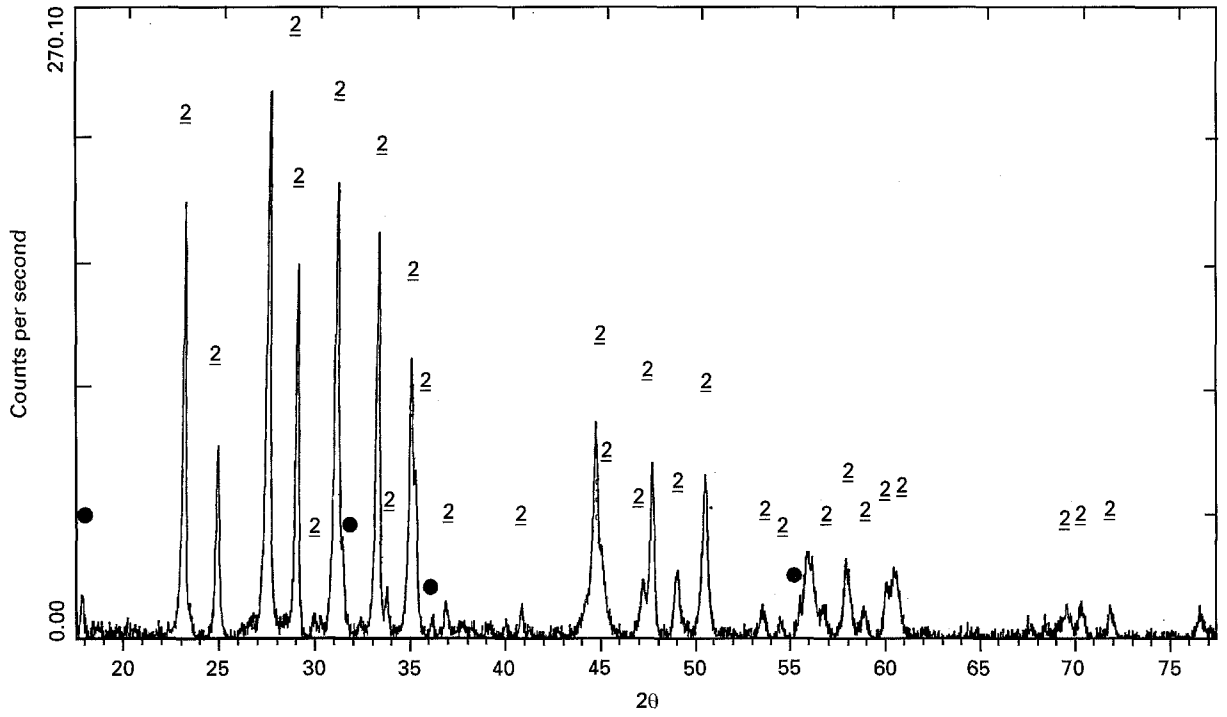

Figure 7 XRD-pattern of the 216 h post annealed sample. 2: 2212 phase; ●: 451 phase.

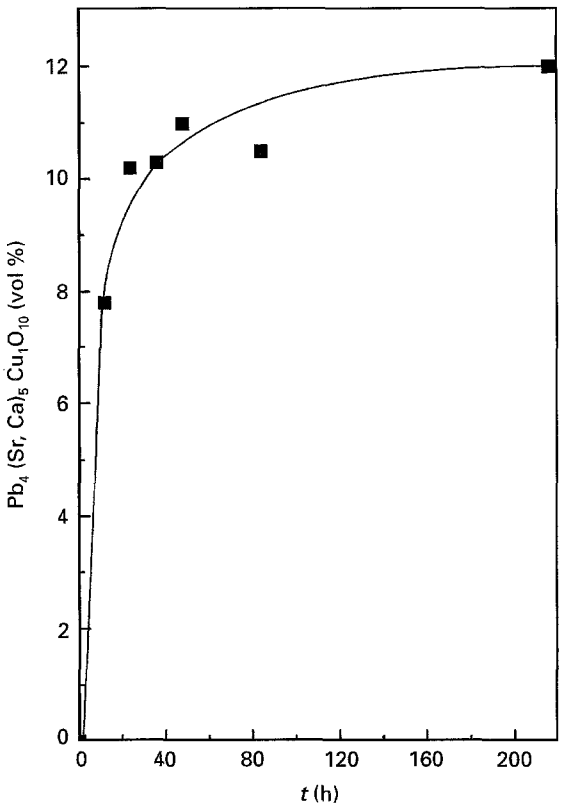

Figure 8 The volume content of the 451 phase versus the post-annealing time at 800 °C.

pinning. An increase of the intragrain current can be provided by pinning, even, but also by an increase of the grain size of the superconducting phase. Therefore, from the physical point of view it cannot be distinguished whether the observed increases of J_c with annealing are due to an increase of pinning or due to an increase of the grain size or the size of clusters of grains of the 2212 phase. However, from the materials science point of view it appears unreasonable that the grain size increases at the beginning of annealing and decreases with annealing, again. In addition, an increase of the grain size of the 2212 phase has not been observed by optical and electron microscopy. Taking these considerations into account the observed increase of J_c is believed to express improved pinning properties of the ceramics.

It is emphasized, that the maximum pinning of the samples is observed, when the precipitation of the secondary phase is not finished. Therefore, it might be concluded, that the introduction of pinning centres in the samples is combined with the precipitation of the secondary phase and, that the precipitates are the pinning centres. However, assuming that point defects, e.g. oxygen vacancies, still are effective pinning centres at 30 K, it is believed that they cannot be the reason for the observed increase of J_c, because all samples were furnace cooled to room temperature after post annealing at 800 °C. Therefore, the density of the point defects are believed to be almost the same in all the samples.

One indication for the conclusion that the precipitates are the introduced pinning centres is that pinning of the prepared samples decreases when the precipitation of the phases have finished and only grain coarsening of the 451 phase crystals occurs, because the efficiency of three-dimensional pinning centres (secondary phases, pores, etc.) decreases with increasing size of the pinning centres [16–22]. However, the J_c of the prepared samples is not maximum at the beginning of precipitation when the precipitates are very small. Therefore, beside the size of the precipitates, the amount of precipitates appears to be important for increasing the overall pinning of the ceramics which is indicated by the increase of the pinning with

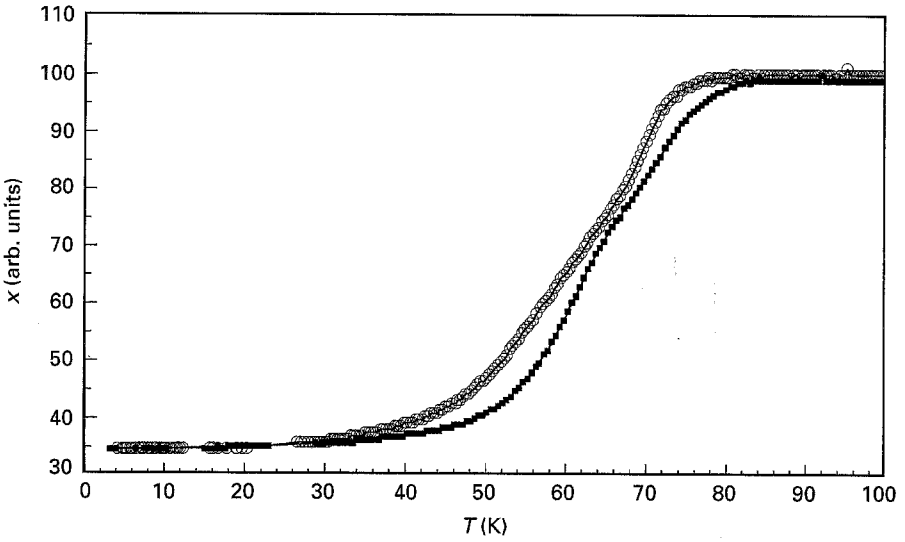

Figure 9 Susceptibility versus temperature plot of the as-sintered sample (○) and the 24 h annealed sample (■).

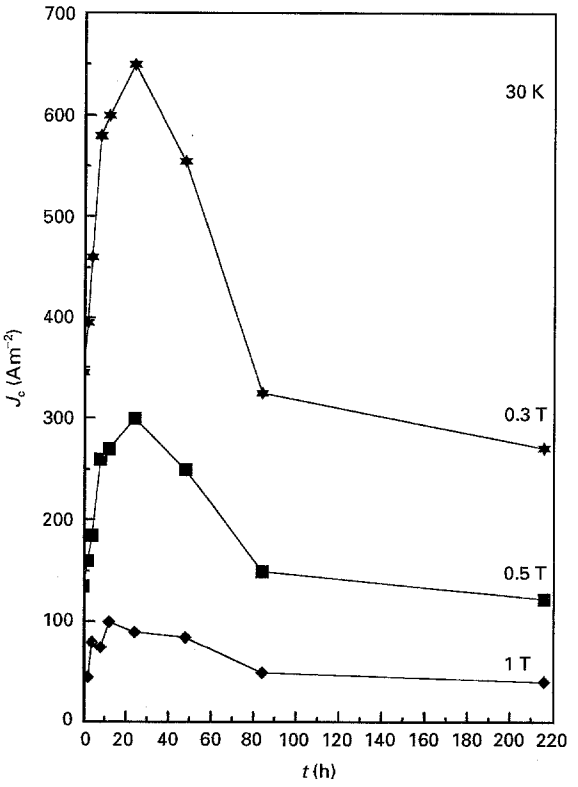

Figure 10 J_c at 30 K versus the post-annealing time of the samples. (★): 0.3 T; (■): 0.5 T, (◆): 1 T.

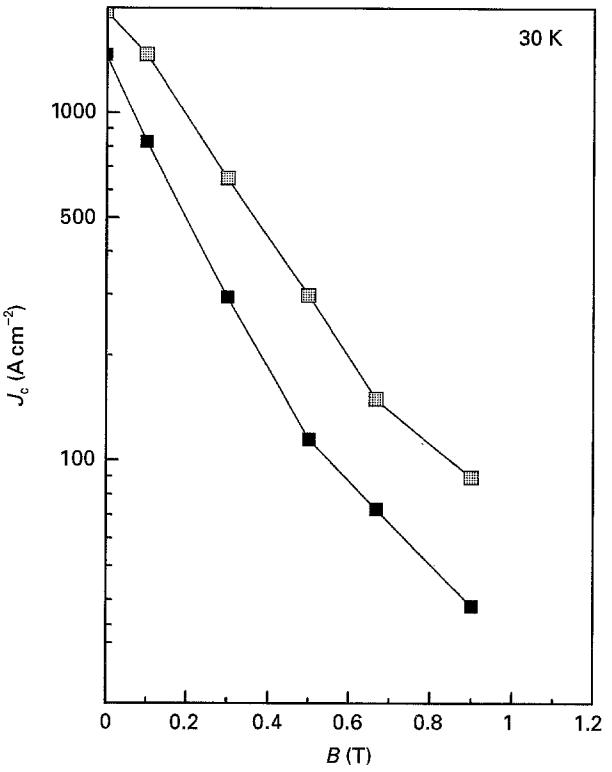

Figure 11 J_c versus the applied magnetic field at 30 K of the as-sintered sample (■) and the 24 h post-annealed sample 20 h (▦).

increasing volume content of the precipitated secondary phase at the beginning of precipitation. Therefore, it can be concluded that maximum pinning is maintained when the ratio of the size and the amount of the precipitates is a maximum. Considering this, maximum pinning of the ceramics can be achieved when the amount of nuclei of the precipitated secondary phases are maximum.

5. Conclusion

In conclusion it is emphasized that the critical current density of high-temperature superconducting 2212 ceramics can be increased by precipitation of secondary phases using the temperature-dependent solubility of Pb. This increase is believed to express improved pinning properties of the superconducting ceramics, in particular an increased pinning energy, which reduces the probability for thermally activated depinning. The introduced pinning centres appear to be the precipitated secondary phases. The maximum increase of the pinning force of the ceramics by the presented processing route is maintained when the ratio of the size and the amount of the precipitates has an optimum value. Due to the fact that comparable results were obtained by precipitation of secondary phases in Ca- and

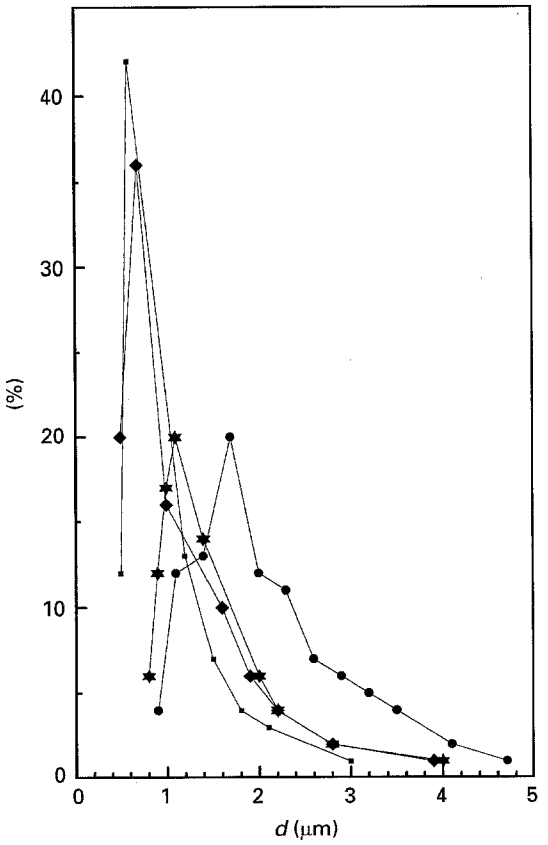

Figure 12 Grain size distribution curves of the 4 5 1 phase. (■): 12 h; (◆): 24 h; (★): 48 h; (●): 216 h.

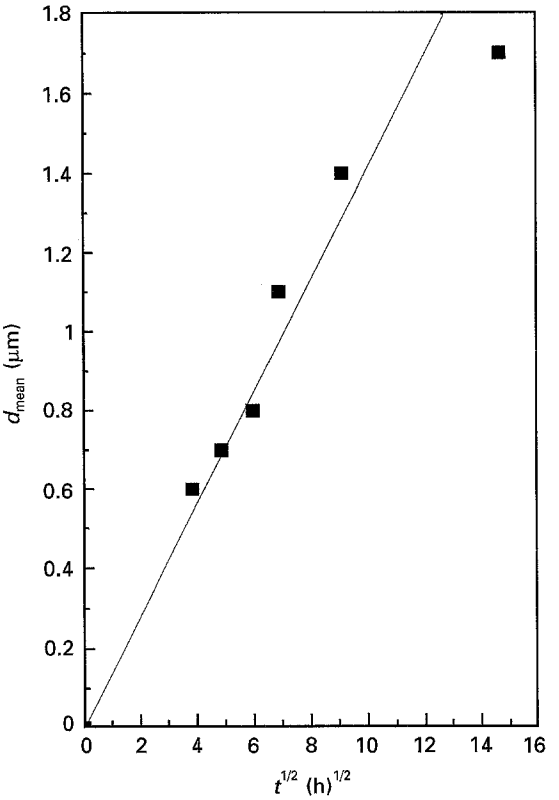

Figure 14 The mean grain size of the 4 5 1 phase versus the square root of the annealing time.

Figure 13 TEM image of a 4 5 1 phase precipitate (black) within 2 2 1 2 phase matrix (grey).

Sr-rich 2 2 1 2 phase ceramics it is believed that precipitation is an effective method to increase the pinning in Bi-based high-T_c superconductors.

References

1. H. KRAUTH, K. HEINE and J. TENBRINK, in "High-Temperature Superconductors–Materials Aspects", edited by H. C. Freyhardt, R. Flükiger and M. Peuckert (DGM, Oberursel, FRG, 1991) p. 29.
2. K. TOGANO, H. KUMAKURA, H. MAEDA and J. KASE, in "Chemistry of High Temperature Superconductors", edited by C. N. R. Rao (World Scientific, London, 1991) p. 399.
3. J. BOCK, S. ELSCHNER and E. PREISLER, in "Advances in Superconductivity III", Proceedings of the ISS 1990, Sendai, edited by K. Kajimura and H. Hayakawa (Springer Verlag, Tokyo, 1991) p. 797.
4. S. GAUSS, Dissertation, University of Karlsruhe, 1987.
5. R. FLÜKIGER, "Advances in Materials Sciences and Engineering" (Pergamon Press, Oxford, 1991).
6. D. J. MILLER, S. SENGUPTA, J. D. HETTINGER, D. SHI, K. E. GRAY, A. S. NASH and K. C. GORETTA, *Appl. Phys. Lett.* **61** (1992) 2823.
7. M. MIRONOVA, D. F. LEE and K. SALAMA, *Phys. C* **211** (1993) 188.
8. V. HARDY, D. GROULT, M. HERVIEU, J. PROVOST, B. RAVEAU and S. BOUFFARD, *Nucl. Instr. Meth.* **B54** (1991) 472.
9. L. CIAVALE, A. D. MARWICK, R. WHEELER, M. A. KIRK, W. L. CARTER, G. N. RILEY Jr and A. P. MALOZEMOFF, *Phys. C* **208** (1993) 137.
10. P. KUMMETH, H.-W. NEUMÜLLER, G. RIES, M. KRAUS, S. KLAUMÜNZER and G. SEEMANN-ISCHENKO, *J. Alloys Compos.* **195** (1993) 403.
11. L. R. MOTOWIDLO, B. A. ZEITLIN, X. S. LING, N. D. RIZZO, J. D. McCAMBRIDGE and D. E. PROBER, in "Processing of Long Lengths of Superconductors", edited by U. Balachandran, E. W. Collings and A. Goyal (TMS, Warrendale, 1994) p. 333.
12. M. MURAKAMI, H. FUJIMOTO, T. OYAMA, S. GOTHO, Y. SHIOHARA, N. KOSHIZUKA and S. TANAKA, in "High-Temperature Superconductors–Materials Aspects", edited by H. C. Freyhardt, R. Flükiger and M. Peuckert (DGM, Oberursel, Germany, 1991) p. 13.

13. M. MURAKAMI, H. FUJIMOTO, S. GOTHO, K. YAMAGUCHI, N. KOSHIZUKA and S. TANAKA, *Phys. C* **185–189** (1991) 321.
14. D. SHI, M. S. BOLEY, U. WELP, J. G. CHEN and Y. LIAO, *Phys. Rev. B*, **40** (1989) 5255.
15. T. UEMURA, K. EGAWA, S. KINOUCHI, M. WAKATA and S. UTSUNOMIYA, *Phys. C* **185–189** (1991) 2219.
16. J. R. CLEM, *Phys. Rev. B* **43** (1991) 7837.
17. E. H. BRANDT, *Phys. C* **195** (1992) 1.
18. *Idem, ibid. Phys. Rev. Lett.* **69** (1992) 1105.
19. *Idem, ibid. Europhys. Lett.* **18** (1992) 635.
20. *Idem, Ibid. Int. J. mod. Phys. B* **5** (1991) 751.
21. J. BOIKO, P. MAJEWSKI and F. ALDINGER, *Phys. Status Solidi (b)* **184** (1994) 417.
22. *Idem, Z. Metallkde* **85** (1994) 100.
23. *Idem, Cryst. Res. Technol.* **29** (1994) 1109.
24. *Idem, Phys. Status Solidi (b)* **187** (1995) K17.
25. D. FEINBERG, *Phys. C* **194** (1992) 126.
26. P. MAJEWSKI, B. HETTICH, S. ELSCHNER and F. ALDINGER, *Appl. Supercond.* **2** (1994) 93.
27. P. MAJEWSKI, H. BESTGEN, S. ELSCHNER and F. ALDINGER, *Z. Metallkde* **80** (1995) 563.
28. P. MAJEWSKI, S. ELSCHNER and F. ALDINGER, *J. Electron. Mater.* **24** (1995) 1937.
29. *Idem, Phys. C* **249** (1995) 241.
30. C. P. BEAN, *Phys. Rev. Lett.* **8** (1962) 250.
31. S. X. DOU, H. K. LIU, Y. L. ZHANG and W. H. BLAN, *Supercond. Sci. Technol.* **41** (1991) 203
32. H. KITAGUCHI, J. TAKADA, K. ODA and Y. MIURA, *J. Mater. Res.* **5** (1990) 1397.
33. P. MAJEWSKI, H.-L. SU, S. KAESCHE and F. ALDINGER, *Phys. C* **221** (1994) 295.
34. S. KAESCHE, P. MAJEWSKI and F. ALDINGER, *J. Electron. Mater.* **24** (1995) 1829.

Received 28 April
and accepted 4 October 1995